Semi-automatic calcium scoring in CT-scans

Sofía Gutiérrez Santamaría

ABSTRACT

Vascular calcification is the pathological deposition of calcium in vascular structures and it is considered a complication of atherosclerosis. Vascular calcium detection by Computed Tomography (CT) can be used as a clinical marker of atherosclerosis. Nowadays, calcium scoring is mainly based on the Agatston method, although there are others based on the volume or mass of the calcifications.

In this study, semi-automatic functionalities are implemented in a new calcium-scoring software application based on MeVisLab with the sole purpose of saving radiologists time in their clinical practice. On the one hand, the interpolation of calcification segmentations have been implemented and on the other hand, the Agatston and volume scores have been computed. For its assessment, the results obtained are compared with those from imageXplorer, the software used so far, which is considered the "gold standard" in this study.

For the interpolation of calcification segmentations, Dice coefficients that compare the similarity between the segmentations performed in imageXplorer and MeVisLab were calculated. The values obtained before using the editing modes fall in the range $[2.3 \cdot 10^{-4} - 0.7]$ and those obtained afterwards are in the range [0.8 - 1.0]. As for the computation of the calcium scores, a Student t-test between the calcium scores from imageXplorer and MeVisLab was conducted. For both the Agatston Score ($t_{32} = 0.03$, $p = 0.97$) and the volume score ($t_{32} = 0.04$, $p = 0.96$) not statistically difference was found. Both the interpolation of calcification segmentations and the computation of the calcium scores are validated, although some future improvements are suggested.

I. INTRODUCTION

A. Vascular Calcification

Vascular calcification is the pathological deposition of calcium in vascular structures [1]. It is associated with several cardiovascular pathological features, including hypertension, congestive heart failure, cardiac hypertrophy, ischemia and increased risk of myocardial infarction and stroke [2] [3]. Thus, calcifications are a significant risk factor for morbidity and mortality in cardiovascular disease [4] [5] [6] [7] [8] [9] [10] [11].

In general, arterial calcification occurs in the intimal layer of the wall and in the aortic valve. Both vascular and cardiac valve calcification are considered complications of atherosclerosis [2] [3] because risk factors that predispose and/or potentiate plaque formation may also predict progression of calcification [12] [13] [14].

Atherosclerosis is a slow-progressing and complicated systemic disease in which fatty substances are deposited in the wall of arteries [1] [15]. This process is described below.

Cholesterol circulate in the bloodstream. The most important of these, the Low Density Lipoprotein (LDL), can migrate through the endothelium and accumulate in the intima. There, the LDL binds proteoglycans of the extracellular matrix; this is a structure consisting of among other things, collagen and elastin that supports cells. On site, the LDL undergoes two chemical changes, namely oxidation and glycosylation. The resulting reaction products contribute further to the process of atherosclerosis [16].

The second step consists of attracting leukocytes (mainly monocytes and lymphocytes) to places where the chemically altered LDL is in the intima. They are attracted by the modified LDL itself, by certain cytokines and monocyte chemoattractant protein-1 (MCP1). If blood flows normally, this does

not happen so quickly, because nitric oxide (NO) is then produced (shear stress related). This has anti-inflammatory properties, as a result of which, among other things, the leukocytes attach less to the vascular wall and LDL can migrate less easily through the endothelium. However, in areas where the blood flow is altered no or less NO is produced. Therefore, more atherosclerosis occurs at these areas [17].

Once in the intima, the monocytes change into macrophages. These have the possibility to incorporate the LDL; they then become foam cells (histiocytes). The foam cells cause an inflammatory process by releasing cytokines, such as interleukin-1 and tumour necrosis factor-alpha, which attract even more macrophages. A number of the foam cells will die off (apoptosis) and form the core of the atherosclerotic plaques. In addition, the content of the foam cells is released, which further contributes to the inflammatory process. Due to the inflammation smooth muscle cells (SMC) migrate from the surrounding layer (the tunica media) to the plaque (intima). In the plaques are also activated T-cells that can make interferon-gamma, which stimulates smooth muscle cells to multiply [18].

In an advanced stage calcium accumulates, as shown in figure 1. What happens to the calcium in the plaque (calcification) shows similarities with bone formation. This makes the plaque 4-5 times as stiff as without the calcification. The calcification serves as a barrier to protect against further inflammatory reactions that aggravate atherosclerosis. In the age of 60-69 years, calcifications occur in 75% of people without vascular problems, and in 100% of 60-69 year-olds with artery disease [15].

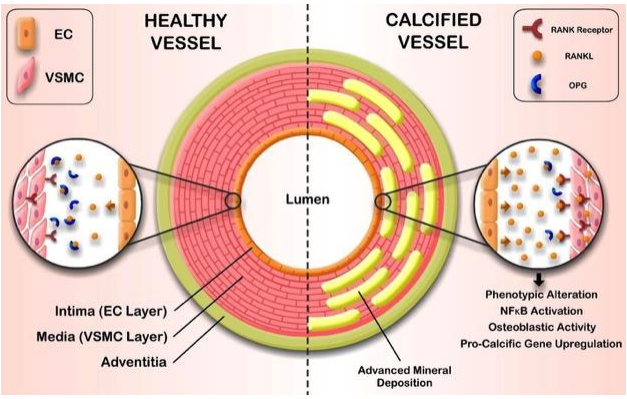

Figure 1. Vascular calcification. Source: (Harper et al., 2016). Published with permission

A vulnerable plaque is a kind of atheromatous plaque –a collection of white blood cells (primarily macrophages) and lipids (including cholesterol) in the wall of an artery– that is particularly unstable and prone to produce sudden major problems such as a heart attack or stroke [19].

The defining characteristics of a vulnerable plaque include but are not limited to: a thin fibrous cap, large lipid-rich necrotic core, increased plaque inflammation, positive vascular remodelling, increased vasa-vasorum neovascularization, and intra-plaque haemorrhage [20].

These characteristics together with the usual hemodynamic pulsating expansion during systole and elastic-recoil-contraction during diastole contribute to a high mechanical stress zone on the fibrous cap of the atheroma, making it prone to rupture [20].

B. Agatston Score

Vascular calcium detection by Computed Tomography (CT) can be used as a clinical marker of atherosclerosis. Nowadays, calcium scoring is mainly based on the Agatston method which is mostly used for coronary arteries [3].

In order to determine the Agatston score, the threshold for a calcific lesion is set at a CT density of 130 Hounsfield units having area ≥ 1 mm^2. Next, a Region Of Interest (ROI) is placed around all lesions found. Subsequently, automated measurements of the lesion area and the maximal CT number of each ROI are recorded [21].

Thereafter, a lesion score is determined based on the maximal CT number in the following manner: 1 = [130 - 199], 2 = [200 - 299], 3 = [300 - 399] and 4 $\geq$400. Then, a score for each ROI is calculated by multiplying the density score and the area. Finally, a total coronary calcium score is calculated by adding up each of the ROI scores [21].

From a clinical perspective, there are some reasons for wanting to improve calcium scoring in CT scans. The current method primarily focus on CT of the coronaries and not on other vascular structures. Besides that, big differences have been found in calcium scores when comparing the various existing platforms [22] [23] [24].

C. Goal

Calcium-scoring is a software application for interactive analysis of radiographs of the vessels, based on imageXplorer [25], developed at the Image Sciences Institute, Utrecht, The Netherlands.

However, the imageXplorer [25] software was implemented in C++, an increasingly unused programming language, and it was created in 1997, which makes the software obsolete. For the aforementioned problems, this software is difficult to maintain at present.

For this reason, this project focuses on the further implementation of a new calcium-scoring software application based on MeVisLab [26]. This will enable new functionalities to be built on top of what already exists, allowing the use of semi-automated tasks, thus saving time for clinicians.

II. MATERIALS AND METHODS

A. Materials

i. Data

CT scans were acquired from six Pseudoxanthoma Elasticum (PXE) patients at the University Medical Center Utrecht (UMCU). PXE is a genetic disease characterized by fragmentation and progressive calcification of elastic fibers in the skin, eyes and blood vessels1. The most common vascular manifestations are peripheral arterial disease (PAD) and increased risk of cerebral infarction [27].

ii. imageXplorer

Moreover, Agatston and volume scores for all the calcifications and their respective segmentations were provided by clinicians at the UMCU. They were obtained from imageXplorer [25], which will be referred as the “gold standard” for comparison purposes.

iii. MeVisLab

MeVisLab [26] represents powerful modular framework for image processing research and development with a special focus on medical imaging. It allows fast integration and testing of new algorithms and the development of clinical application prototypes.

In the present study, this software has been used to improve the graphical interface of the calcium-scoring application and to implement a range of semi-automatic functions.

iv. GitLab

With the aim of ensuring changes in the application could be tracked with full transparency and consistency, GitLab [28] has been used. A new branch called “sofia” was created to accommodate all new contributions.

GitLab [28] is a platform that maximizes the overall return on software development by delivering software faster and efficiently, while strengthening security and compliance.

v. MATLAB

For the purpose of contrasting the results obtained with MeVisLab [26] and those obtained with the "gold standard", some scripts have been coded in MATLAB [29].

MATLAB [29] is a numerical computing system that provides an integrated development environment with its own programming language.

Among its basic capabilities are the manipulation of arrays, the representation of data and functions, the implementation of algorithms, the creation of user interfaces, and communication with programs in other languages and with other hardware devices.

B. Methods

i. Interface Layout

With the aim of using this application in clinical practice, the calcium-score graphical interface was improved to give it a more formal appearance and make it more user-friendly.

To this end, buttons were added and regrouped into different sections. All these changes were implemented in the MeVisLab editing script.

The interface layout was evaluated by two radiologists from the UMCU by means of a questionnaire. This consisted of five questions, as illustrated in figure 2, following a Likert scale where 1 meant strongly disagree and 5 strongly agree.

1. The interface is user-friendly
2. The displayed information is complete
3. The program is easy to use
4. The application is useful
5. The software should be incorporated into the clinic

Figure 2. Graphical interface questionnaire

ii. Slice Interpolation

Slice interpolation of calcium segmentations was implemented making use of the MeVisLab module CSOSliceInterpolator.

This module generates interpolated contours for existing CSOs that are parallel on z-slices. The interpolation itself is done by establishing a spline surface function out of the path points of the contours and then scanning the missing slices in between by a marching squares algorithm.

There are two values to adjust computation speed and quality, the Max Num Points For Function and the Spline Quality. The first one sets a fixed maximum border for the amount of points that are taken into account in the generation of the spline function for one section. The second one is a relative factor for determining the resulting amount of points. In this work, Max Num Points For Functions was set to 500 and Spline Quality to 1, the maximum, although that meant sacrificing computing speed.

The evaluation of the interpolated segmentations was assessed by means of a comparison with imageXplorer results through the calculation of the Dice similarity coefficient.

iii. Calcium Scores Computation

The computation of the calcium scores was implemented as described in the paper by Agatston et al. [21]. To that end, the CT scans were converted into NumPy arrays, the segmentations were voxelized to be used as CSOs masks and the voxel size was taken into account.

The evaluation of the scores was assessed based on a comparison with the "gold standard" results by means of a Student t-test, using a p-value of 0.05 as the threshold for statistical significance.

Figure 3. Calcium-scoring application graphical interface

III. RESULTS

A. Interface Layout

The final layout of the calcium-score application is shown in figure 3. Apart from the main viewer and the ortho viewer 2D, five sections are displayed: files, anatomy, edit modes, automatic modes and scores.

In the files section, four buttons can be found. Two buttons to open the CT file (.mhd) and the contour file (.cso) and another two to save the segmentation (.nii.gz) and the segmentation contour (.cso), respectively.

Just below is the anatomy section, which allows to choose the area of the body (head and neck, heart, aorta, arms, breast, abdominal, pelvis or legs) where a calcification has been detected. Additionally, for each region, there is another tab that enables to select the specific artery. For instance, in the legs group, four subgroups can be selected: left and right popliteal artery and left and right femoral artery. It should be mentioned that a different colour is used for the segmentations within each subgroup.

Next is the editing section in which you can choose between the following edit modes to segment the calcifications: contour, slice/move, spline and bulge. The first one follows the contours of the thresholded image automatically, based on the threshold value if enabled. It should be noted that the threshold can be displayed, as shown in figure 4.

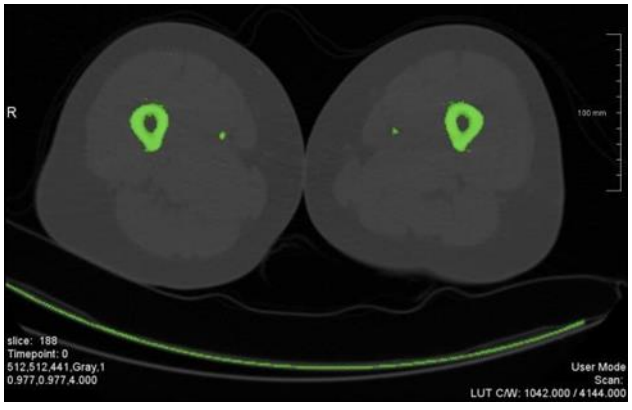

Figure 4. Displayed threshold ≥130 Hounsfield units

The second editing mode slices existing contours by clicking and dragging the cursor across one. The third one creates a smooth curve between placed control points and the last one adjusts the segmentation by pushing or pulling existing contours. Two parameters can be modified in order to detect the contour: selection distance and influence length.

The automatic modes section was built from scratch. Two subsections were implemented: propagate the segmentation and delete the Contour Segmented Objects (CSOs). When propagating the segmentation, the start and end CSOs have to be selected before clicking the "Interpolate Slices" button. As to the elimination of the CSOs, two different options can be chosen: delete the CSOs from a selected group and subgroup or delete the CSOs from all groups.

Finally, the scores section was designed to visualize the Agatston and volume scores for the segmented calcifications. The Agatston score reflects the total area and density of calcium deposits, while the volume score reflects the total volume of calcium deposits.

B. Slice Interpolation

Two different Dice scores have been obtained to evaluate each propagation of the calcification segmentations. Both scores compare the segmentations performed by two healthcare professionals using imageXplorer with the segmentations obtained using MeVisLab. However, the difference between the scores lies in the type of segmentation performed in MeVisLab. The first segmentation is the straightforward result of interpolating between the first and last slice of the same calcification, whereas the second one has been improved by using the editing modes of the application.

As presented in table 1, the Dice scores obtained for the first case are very disparate, oscillating in the range $[2.3 \cdot 10^{-4} - 0.7]$. However, after adjusting some segmentations, an increase in the scores can be noticed, reaching values between [0.8 - 1.0].

C. Calcium Scores Computation

When comparing imageXplorer and MeVisLab in the calculation of the Agatston and volume scores, not statistically significant difference was found ($t_{32} = 0.03$, $p = 0.97$) ($t_{32} = 0.04$, $p = 0.96$), respectively.

Furthermore, after calculating the difference between the calcium scores obtained with both softwares, it was observed that with imageXplorer the results are slightly higher than with MeVisLab, as the mean differences of the Agatston and volume scores obtained are 7.48 and 7.38, respectively.

Table 1. Calcium scores and Dice similarity coefficient scores for every calcification

			imageXplorer		MeVisLab		
Patient	**Slices with calcifications**	**Label**	**Agatston Score**	**Volume Score**	**Agatston Score**	**Volume Score**	**Dice Score**
PXE003_PT_20130903_63407_3	95	POP_L	16.5	30.5	13.0	23.0	×
	96						
	156	FEM_R	61.0	57.2	61.0	57.0	×
	157						
	172	FEM_L	239.1	179.3	234.0	175.0	$2.5 \cdot 10^{-4}$ ↓ 0.9
	173						
	174						
	175						
	213	IIA_R	1.3	3.8	1.0	4.0	×
	332	LAD	15.3	26.7	13.0	23.0	×
	333						
PXE004_CT_20220119_23495_202	187	POP_L	218.7	164.0	193.0	145.0	0.5 ↓ 0.9
	188						
	189						
	250	FEM_L	509.9	385.3	448.0	336.0	$2.3 \cdot 10^{-4}$ ↓ 0.8
	251						
	252						
	253						
	254						
PXE079_CT_20200207_26484_202	104	POP_R	53.4	72.5	47.0	53.0	0.1 ↓ 1.0
	105						
	106						
	107						
	112	POP_L	109.4	95.4	109.0	95.0	0.1 ↓ 0.9
	113						
	114						
	115						
PXE095_CT_20220126_25693_202	144	POP_R	254.3	202.2	256.0	202.0	0.5 ↓ 1.0
	145						
	146						
	147						
	166	POP_L	564.6	423.4	565.0	423.0	0.7 ↓ 1.0
	167						
	168						

	217	FEM_L	1103.7	827.8	1099.0	824.0	0.7 ↓ 1.0
	218						
	219						
	220						
	221						
	222						
	223						
PXE355_CT_20200527_21255_202	188	POP_L	1383.5	1037.6	1378.0	1034.0	0.7 ↓ 1.0
	189						
	190						
	191						
	192						
	197	FEM_R	824.0	618.0	824.0	618.0	0.8 ↓ 1.0
	198						
	199						
	229	FEM_L	2379.1	1792.9	2375.0	1781.0	0.7 ↓ 1.0
	230						
	231						
	232						
	233						
	234						
PXE406_CT_20220112_33003_202	179	FEM_L	315.3	236.5	315.0	237.0	0.7 ↓ 1.0
	180						
	181						
	200	FEM_R	447.9	331.0	443.0	332.0	0.7 ↓ 1.0
	201						
	202						
	203						
	204						
	205						

IV. DISCUSSION

A. Evaluation

i. Interface Layout

Table 2 displays the answers to the questionnaire on the graphical interface. As can be seen, there is mutual agreement among the experts that the interface is user-friendly, the information displayed is complete and that the application is useful.

However, the ease of use of the programme and its incorporation into clinical practice is controversial. On the one hand, the former can be solved by creating a user manual for the application. On the other hand, the latter can be addressed by implementing a series of improvements mentioned in the "Future Improvements" section.

Table 2. Graphical interface questionnaire answers

Question	Answer
The interface is user-friendly	4
The displayed information is complete	4
The program is easy to use	3.5
The application is useful	4
The software should be incorporated into the clinic	3.5

ii. Slice Interpolation

The interpolation between calcium segmentations in different slices was influenced by two variables: the size and morphology of the calcifications. To study their relationship, the correlation coefficient between the Dice scores and each of the variables was calculated.

On the one hand, it was found that the larger the calcifications, the better the Dice scores ($r_{11} = 0.64$, $p = 0.02$). On the other hand, the greater the irregularity of the calcifications, the worse the Dice scores ($r_{11} = -0.37$, $p = 0.21$). This explains the Dice score results in the order of 10^{-4} obtained in patients PXE003_PT_20130903_63407_3 and PXE004_CT_20220119_23495_202, as they had the most irregular and smallest calcifications.

The influence of these two variables is due to the fact that the MeVisLab module that performs the interpolations only takes into account the contour of the calcifications. Thus, if the calcification is very small, the contour is not well defined and, therefore, the interpolation is poor. Likewise, when the calcification is very irregular, the contour of the calcification in one slice and in the immediately subsequent one vary greatly, causing the interpolation to fail, as shown in figure 5.

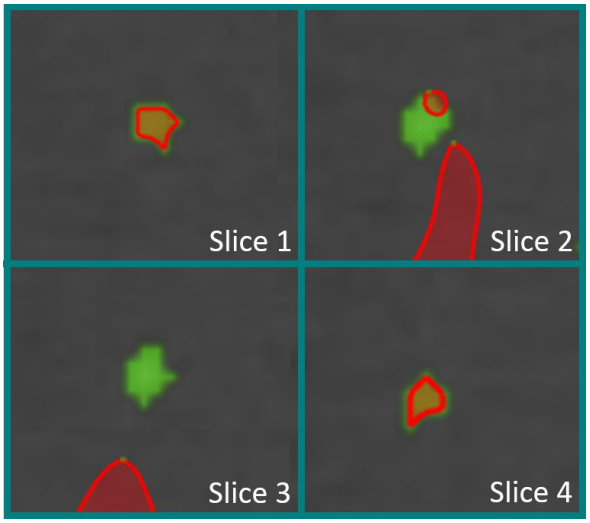

Figure 5.Interpolation failed

iii. Calcium Scores Computation

According to the results of the Student t-test, there are not significant differences regarding the calcium scores between the two softwares, so it can be stated that the scores obtained with MeVisLab are similar to those obtained by the "gold standard".

However, in order to investigate why the calcium scores obtained with imageXplorer are slightly higher than those obtained with MeVisLab, differences in the segmentations obtained by imageXplorer and MeVisLab were calculated.

As expected, the differences lie at the edges of the calcifications. This is because with MeVisLab the areas of the segmented calcifications are smaller as the contour-based segmentations are more precise than those based on a threshold.

Figure 6 depicts the difference between the segmentations of the two softwares for a given calcification. The pixels that have been segmented by imageXplorer but not by MeVisLab are shown in white and are the reason for the higher calcium scores.

Figure 6. Difference between imageXplorer and MeVisLab calcification segmentations

In addition, Bland-Altman plots have been created to analyse the agreement between the two softwares used to obtain the calcium scores, as shown in figures 7 and 8.

The mean difference is close to 0 in both cases, so no bias seems to exist. Furthermore, the differences within mean ± 1.96 SD are not clinically important, so the two softwares can be used interchangeably to calculate the calcium scores.

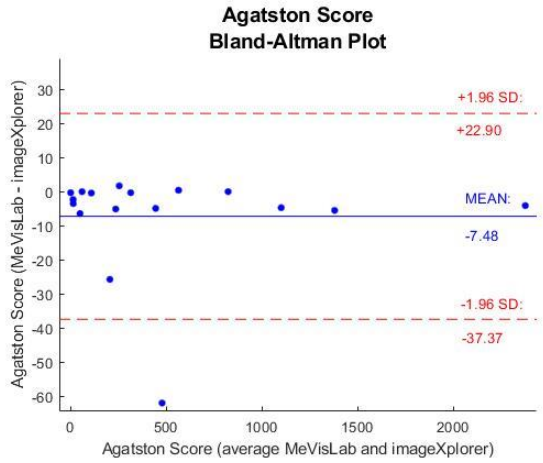

Figure 7. Bland-Altman plot for the Agatston score

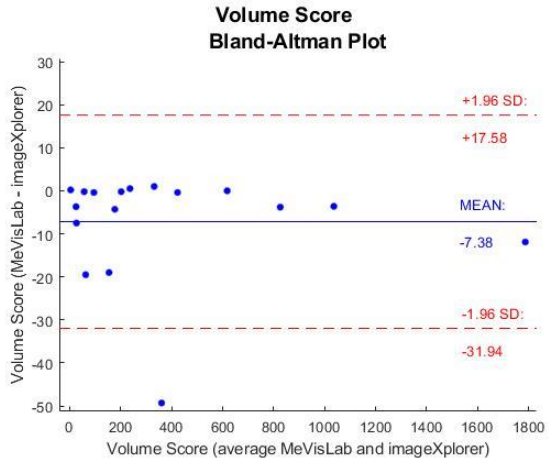

Figure 8. Bland-Altman plot for the volume score

B. Future Improvements

i. Interface Layout

One improvement that could be made to the graphical interface is the addition of more arteries within each anatomical group in order to provide more specific calcium scores per area.

Another suggestion is to display the calcium scores by groups in a table, instead of the total as is currently done.

ii. Slice Interpolation

As previously mentioned, the module CSOSliceInterpolator only takes into account the contour of the calcifications to perform the interpolations.

Therefore, it would be very interesting to combine both the contour and a threshold ≥130 Hounsfield units to perform the interpolation. Furthermore, depending on the size and morphology of a given calcification, greater or lesser weight could be given to each of these two parameters in order to improve the interpolation in each case.

iii. Calcium Scores Computation

According to de Jong et al. [22], van der Star et al. [23] and Willemink et al. [24], the traditional Agatston score has important limitations, including suboptimal reproducibility, which results in subjects being incorrectly risk classified.

For this reason, it is necessary to develop another quantification method for vessel calcifications.

iv. Addressing Partial Volume Effect (PVE)

A limitation of the current segmentations is that, although they are contour-based, they are voxelized when saving them. Therefore, the advantage of obtaining very precise segmentations is lost due to PVE.

One solution would be, on the one hand, to count the number of pixels that are part of the calcification edges and, on the other hand, to calculate the area of the segmentation before it is voxelized.

This way, when saving the segmentation, the pixels of the edges of the calcification could be reduced until the previously calculated area is obtained.

v. DICOM Files

Last but not least, the CT scan files that are opened from the application must have an .mhd extension, which stands for MetaImage MetaHeader.

However, the files generated in clinical practice after a CT scan are in DICOM format, which stands for Digital Imaging and Communications in Medicine. Therefore, an intermediate step would be omitted if DICOM files could be opened directly from this application.

V. CONCLUSIONS

The implementation of the calcium-scoring application in MeVisLab has a lot of potential due to its ability to build new functionalities on top of what already exists, allowing the use of semi-automated tasks, which will save a lot of time for clinicians.

A clear example of this is the implementation of the interpolation of calcification segmentations. Until now, radiologists had to select calcifications slice per slice, which is a rather tedious task. However, with this application, it is sufficient to select the start and end of a calcification to have it segmented in all the slices in which it appears. Furthermore, with the incorporation of an interpolation based on both the calcifications contours and a threshold ≥130 Hounsfield units, these interpolated segmentations will not require the use of editing modes to adjust them.

Additionally, the display of the calcium scores at the same time as the CT scans are being visualised makes it easier for clinicians to make a diagnosis. New calcium scores addressing the limitations of the current ones will be crucial for this application to be implemented in clinical practice.

VI. REFERENCES

[1] J. Shao, S. Cheng, J. Pingsterhaus, N. Charlton-Kachigian, A. Loewy y Towler D.A., «Msx2 promotes cardiovascular calcification by activating paracrine Wnt signals,» *The Journal of Clinical Investigation,* vol. 115, pp. 1210-1220, 2005.

[2] L. Demer y Y. Tintut, «Vascular calcification: pathobiology of a multifaceted disease,» *Circulation,* vol. 117, pp. 2938-2948, 2008.

[3] R. Johnson, J. Leopold y J. Loscalzo, «Vascular calcification: pathobiological mechanisms and clinical implications,» *Circulation Research,* vol. 99, pp. 1044-1059, 2006.

[4] A. Tsaousi, C. Mill y S. George, «The Wnt pathways in vascular disease: lessons from vascular development,» *Current Opinion in Lipidology,* vol. 22, pp. 350-357, 2011.

[5] M. Christman, D. Goetz, E. Dickerson, K. McCall, C. Lewis, F. Benencia, M. Silver, L. Kohn y R. Malgor, «Wnt5a is expressed in murine and human atherosclerotic lesions,» *American Journal of Physiology - Heart and Circulatory Physiology,* vol. 294, pp. H2864-H2870, 2008.

[6] Y. Geng, J. Hsu, J. Lu, T. Ting, M. Miyazaki, L. Demer y . Y. Tintut, «Role of cellular cholesterol metabolism in vascular cell calcification,» *Journal of Biological Chemistry,* vol. 286, pp. 33701-33706, 2011.

[7] N. Chen y S. Moe, «Vascular calcification: pathophysiology and risk factors,» *Current Hypertension Reports,* vol. 14, pp. 228-237, 2012.

[8] J. Leopold, «Cellular mechanisms of aortic valve calcification,» *Circulation Cardiovascular Interventions,* vol. 5, p. 605–614, 2012.

[9] J. Wasilewski, K. Mirota, K. Wilczek, J. Glowacki y L. Polonski, «Calcific aortic valve damage as a risk factor for cardiovascular events,» *Polish Journal of Radiology,* vol. 77, pp. 30-34, 2012.

[10] M. van Gils, M. Bodde, L. Cremers, D. Dippel y A. van der Lugt, «Determinants of calcification growth in atherosclerotic carotid arteries: a serial multi-detector CT angiography study,» *Atherosclerosis,* vol. 227, pp. 95-99, 2013.

[11] H. Tsuda, Y. Moritsuchi, F. Almeida, A. Lowe y T. Tsuda, «The relationship between cephalometric carotid artery calcification and Framingham Risk Score profile in patients with obstructive sleep apnea,» *Sleep Breath,* vol. 17, pp. 1003-1008, 2013.

[12] E. Askevold, L. Gullestad, S. Aakhus, T. Ranheim, T. Tonnessen, O. Solberg, P. Aukrust y T. Ueland, «Secreted Wnt modulators in

symptomatic aortic stenosis,» *Journal of the American Heart Association: Cardiovascular and Cerebrovascular Disease,* vol. 1, nº 6, 2012.

[13] P. Poggio, J. Grau, B. Field, R. Sainger, W. Seefried, F. Rizzolio y G. Ferrari, «Osteopontin controls endothelial cell migration in vitro and in excised human valvular tissue from patients with calcific aortic stenosis and controls,» *Journal of Cellular Physiology,* vol. 226, pp. 2139-2149, 2011.

[14] A. Alexopoulos, A. Kaoukis, H. Papadaki y V. Pyrgakis, «Pathophysiologic mechanisms of calcific aortic stenosis,» *Therapeutic Advances in Cardiovascular Disease,* vol. 6, pp. 71-80, 2012.

[15] E. Harper, H. Forde, C. Davenport, K. Rochfort, D. Smith y P. Cummins, «Vascular calcification in type-2 diabetes and cardiovascular disease: Integrative roles for OPG, RANKL and TRAIL,» *Vascular Pharmacology,* vol. 82, pp. 30-40, 2016.

[16] A. Poznyak, A. Grechko, P. Poggio, V. Myasoedova, V. Alfieri y A. Orekhov, «The Diabetes Mellitus-Atherosclerosis Connection: The Role of Lipid and Glucose Metabolism and Chronic Inflammation,» *International Journal of Molecular Sciences,* vol. 21, nº 5, pp. 1835-1845, 2020.

[17] M. Rahman y K. Woollard, «Atherosclerosis,» *Advances in Experimental Medicine and Biology,* vol. 1003, pp. 121-144, 2017.

[18] P. Libby, P. Ridker y G. Hansson, «Progress and challenges in translating the biology of atherosclerosis,» *Nature,* vol. 473, nº 7347, pp. 317-325, 2011.

[19] H. Lu y A. Daugherty, «Atherosclerosis,» *Arteriosclerosis, Thrombosis, and Vascular Biology,* vol. 35, nº 3, pp. 485-491, 2015.

[20] A. Hafiane, «Vulnerable Plaque, Characteristics, Detection, and Potential Therapies,» *Journal of Cardiovascular Development and Disease,* vol. 6, nº 3, pp. 26-36, 2019.

[21] A. Agatston, W. Janowitz, F. Hildner, N. Zusmer, M. Viamonte y R. Detrano, «Quantification Of Coronary Artery Calcium Using Ultrafast Computed Tomography,» *Journal of the American College of Cardiology,* vol. 15, nº 4, pp. 827-832, 1990.

[22] D. de Jong, S. van der Star, R. Bleys, A. Schilham, H. Kuijf, P. de Jong y M. Kok, «Computed tomography-based calcium scoring in cadaver leg arteries: Influence of dose, reader, and reconstruction algorithm,» *European Journal of Radiology,* vol. 146, 2022.

[23] S. van der Star, D. de Jong, R. Bleys, H. Kuijf, A. Schilham, P. de Jong y M. Kok, «Quantification of Calcium in Peripheral Arteries of the Lower Extremities Comparison of Different CT Scanners and Scoring Platforms,» *Investigative Radiology,* vol. 57, nº 3, pp. 141-147, 2022.

[24] M. Willemink, N. van der Werf, K. Nieman, M. Greuter, L. Koweek y D. Fleischmann, «Coronary artery calcium: A technical argument for a new scoring method,» *Journal of Cardiovascular Computed Tomography,* vol. 13, pp. 347-352, 2019.

[25] I. S. Institute, «imageXplorer». Utrecht, The Netherlands Patente Software, 1997-2011.

[26] «MeVisLab». Bremen, Germany Patente Software, 2008.

[27] L. Omarjee, C. Roy, C. Leboeuf, J. Favre, D. Henrion, G. Mahe, G. Leftheriotis, L. Martin, A. Janin y G. Kauffenstein, «Evidence of Cardiovascular Calcification and Fibrosis in Pseudoxanthoma Elasticum Mouse Models

Subjected to DOCA-Salt Hypertension,» *Nature,* vol. 9, nº 16327, 2019.

[28] G. Inc., «GitLab». Patente Software, 2011.

[29] MathWorks, «MATLAB». Patente Software, 1984.